MNRAS 000, 1–11 () Preprint 11 February 2019 Compiled using MNRAS LATEX style file v3.0

Can we predict the impact conditions of meter-sized meteoroids?

Jorge I. Zuluaga[1]★, Pablo A. Cuartas-Restrepo[1], Jhonatan Ospina[2] and Mario Sucerquia[1]
[1]*Solar, Earth and Planetary Physics Group - SEAP, Institute of Physics, University of Antioquia, calle 70 No. 52 - 21, Medellín (Colombia)*
[2]*Sociedad Antioqueña de Astronomía / CAMO group, Medellín (Colombia)*

Accepted XXX. Received YYY; in original form ZZZ

ABSTRACT

A few meter-sized meteoroids impact the atmosphere of the Earth per year. Most (if not all) of them are undetectable before the impact and hence, predicting where and how they will fall, seems to be impossible. In this letter we show compelling evidence that we can constrain, in advance, the dynamical and geometrical conditions of an impact. For this purpose, we analyze the well-documented case of the Chelyabinsk impact and the more recent and smaller Cuba event, whose conditions we additionally estimate and provide here. After applying the *Gravitational Ray Tracing* algorithm (GRT) to theoretically "predict" the impact conditions of the aforementioned events, we find that the speed, incoming direction and (marginally) the orbital elements, can be constrained in advance, starting only on one hand, with the geographical location and time of the impact, and on the other hand, with the distribution in configuration space of Near Earth Objects (NEOs). Any improvement in our capability to predict or at least to constrain impact properties of medium-sized and large meteoroids, will help us to be better prepared for its potentially damaging effects.

Key words: methods: numerical – meteorites, meteors, meteoroids.

1 INTRODUCTION

Earth is impacted by hundreds to thousands of centimeter-sized meteoroids each year. Meter-sized objects are much less frequent, with just a few of them falling into the Earth every year (Brown et al. 2013). Most of these events occur at very high altitudes, so their shock waves never reach the surface. Still, they are detectable by satellites (Chapman & Morrison 1994; Brown et al. 2002) and infrasound detectors (see eg. (Silber et al. 2011)). In a few cases, however, an impact of a meter-sized object (releasing energies in the range of several to hundreds of ktons) may happen over populated areas, posing a real risk over infrastructure and population (Popova et al. 2013; Rumpf et al. 2015).

In the case of large (several hundreds of meters) and well-knwon Near Earth Object (NEOs) whose impact probabilities are not negligible, we can predict in advance where and how the object could impact our planet (Chapman 2004; Chesley 2005; Rumpf et al. 2015). This is possible because the impactor have been previously observed and its orbital elements are very well-constrained.

furthermore, the detection of meter-sized NEOs is slow and difficult (Boslough et al. 2015). Predicting where and how one of these objects will impact our planet at a given time, seems to be an impossible task. Proof of this are the impacts in Chelyabinsk, Benenitra (Madagascar) and recently that of Cuba, which had not been observed prior to the event.

In two recent works, Zuluaga & Sucerquia (2017, 2018) introduced a novel numerical technique, the Gravitational Ray Tracing (GRT), intended (among many potential applications) to compute the probability that at a given time, certain geographical region of the Earth (or any other planetary body) be impacted by an asteroid. More recently Zuluaga et al. (2019) applied GRT to study the impact of a small object against the moon, testing the technique for the first time in a different context and with a different aim for which it was originally devised.

In this letter we apply GRT (Section 4) to study retrospectively the impact conditions (Section 2) of the best documented atmospheric explosion, the Chelyabinsk impact (Section 3), and a recent, smaller, but still energetic event over Cuba. Our aim here is to check if the "predictions" that GRT could make about the incoming direction, speed and orbital element of the potential impactors at the place and time of those events (Section 5), coincide with the observed conditions of the impacts.

Since, to the date of writing, no full reconstruction of the Cuba event has been done (combining infrasound, satellite data and images we expect the atmospheric trajectory and

★ Corresponding author: jorge.zuluaga@udea.edu.co

orbit will be precisely reconstructed soon), we provide our own estimations of the impact conditions as obtained from public footage using the methods in Zuluaga et al. 2013 (Section 6).

2 IMPACT CONDITIONS

We call "impact conditions" to the set of bulk geometrical and dynamical properties of a meteoroid impact.

Meter-sized objects, ie. $\lesssim$ 50 m, hardly achieve to impact the surface. They normally explode at high altitude in the atmosphere (Brown et al. 2002). Detonations happen when the atmospheric density increases and the aerodynamic pressure at the leading edge of the impactor surpass the strength of the material (Hills & Goda 1998). Typical heights of the detonation and the consequent fragmentation (which depends on the strength of the meteoroid) are between 70-20 km (Svetsov et al. 1995; Collins et al. 2005). Usually, a cascade of breakup of the main body can also occur, spreading the material of the meteor over certain area on the planet surface.

We call the intersection between the geoid and a straight line tangent to the atmospheric trajectory of the meteoroid, the "projected impact point", and denote their geodetic coordinates with $\mathrm{lon_{imp}}$, $\mathrm{lat_{imp}}$.

The point in the sky from which the meteoroid seems to come is known as "the impact Radiant". We parameterize the radiant here in terms of the Azimuth (A_{rad}) and elevation (h_{rad}) of the radiant as observed from the projected impact point.

Because of the impact speed v_{imp} (typically between 14-20 km/s) and the fact that the mass of the impactor is larger than the mass of the atmosphere displaced during its penetration, the trajectory of the bolide can be assumed nearly rectilinear until it reaches the upper troposphere. Therefore a precise determination of the *projected impact point* and the *radiant* are key to estimate the heliocentric orbital elements, q, e, i, Ω and ω (with q the perihelion distance, e the eccentricity, i the orbital inclination, Ω the longitude of ascending node and ω the argument of perihelion) of the impactor before its energetic interaction with the Earth's atmosphere.

3 STUDIED EVENTS

In recent years, and especially due to the expansion and densification of urban areas and the availability of cheap and pervasive electronic cameras, there have been two major impact events with a large number of witnesses and footage records: the Chelyabinsk event (February 15, 2013) and the recent Cuba event (February 1, 2019). Other relatively large events, such as one in Madagascar (July 27, 2018), had also thousands of witnessed but much less available imagery and data.

Multiple sources of information, including public footage, satellite imagery and data, and records from infrasound networks, has allowed us to determine with incredible detail (at least in the case of Chelyabinsk impact) the impact conditions of these events.

To the date of writing, no full reconstruction of the Cuba event, combining all the above sources of information, has been still published. In Section 6, we provide our own estimations of the impact conditions of the Cuba event, as obtained from public footage and using the methods in Zuluaga et al. 2013.

Property	Chelyabinsk (2013)	Cuba (2019)
Atmospheric Trajectory		
	Ref. 1	This work
Date	2013/02/15	2018/02/01
Time (UTC)	03:20:20	18:17:10
$\mathrm{lon_{imp}}$ (deg)	+59.8703*	-83.7822
$\mathrm{lat_{imp}}$ (deg)	+55.0958*	+22.8024
A_{rad} (deg)	103.5	179
h_{rad} (deg)	18.55	33.0
v_{imp} (km/s)	19.03	18.00
Heliocentric Orbit		
	Ref. 1	This work
a (AU)	1.72	1.32
e	0.571	0.44
q (AU)	0.738	0.75
i (deg)	4.98	11.68
Ω (deg)	326.459	132.55
ω (deg)	107.67	283.8
P (years)	2.33	1.52
T_p **	2.72	2.78

Ref. 1 Borovička et al. 2013
*Ref. 2 Zuluaga et al. 2013
**Tisserand parameter, $T_p = 1/a + 2\cos i\sqrt{a(1-e^2)}$

Table 1. Impact conditions of the impact events studied in this work.

In Table 1 we show the impact conditions of the Chelyabinsk and Cuba events, as obtained from the available literature (Zuluaga et al. 2013; Popova et al. 2013; Borovička et al. 2013) and from our own estimations (Section 6).

4 GRAVITATIONAL RAY TRACING

Are the impact of meter-sized meteoroids and their conditions predictable? As stated above, the small size of the objects involved on the events studied here, mostly prevent their early detection, rendering very improbable, if not impossible to anticipate their place and conditions of arrival.

Zuluaga & Sucerquia (2017, 2018) (hereafter ZS2018) developed and tested a backward integration technique intended to compute the statistical properties of impact conditions. The technique was inspired in the ray tracing algorithms used in the film and game industries to render photorealistic images (see eg. Comninos 2010 and references there in).

In GRT, we randomly generate N different impact velocities (regularly spaced between the Earth's escape velocity and that of the Solar System as measured at the orbit of our planet) and M random incoming directions, following a blue-noise distribution to avoid aliasing sampling effects (see Section 2.1 in ZS2018). Starting at a given impact site and a desired date and time, we integrate backwards the trajectory of this $N \times M$ test particles in the Solar System

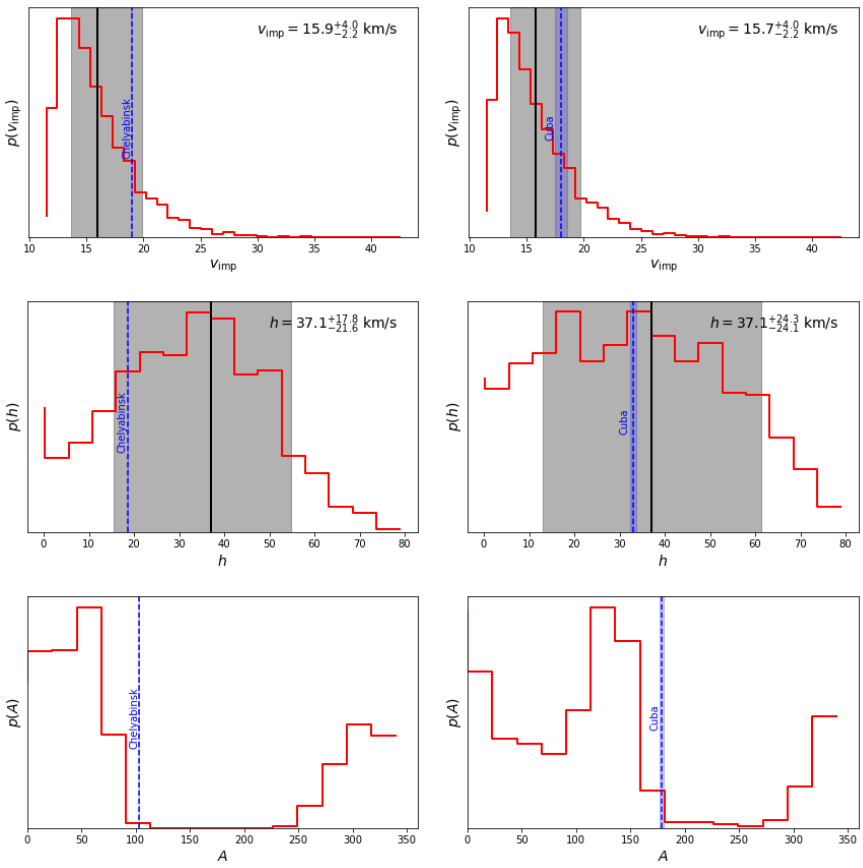

Figure 1. Marginal probability distributions of impact velocity, high and azimuth for Chelyabinsk (left panels) and Cuba (right panels) events.

gravitational field. The integration stops when test particles reach an asymptotic heliocentric orbit.

The probability that a test particle, having impact conditions $(A, z, v_{\rm imp})$, correspond to a real meteoroid, is given by the so-called *ray probability*:

$$P(A, z, v_{\rm imp}; t) \quad \propto \quad f(\theta_{\rm apex}, \lambda_{\rm apex}) R(q, e, i, \Omega, \omega). \qquad (1)$$

Here $R(q, e, i, \Omega, \omega)$ is the number density of NEOs in the orbital elements space. In order to correct for the "defocusing" effect that the relative motion of the Earth has with respect to the NEOs population (see Section 2.5 in ZS2018), we introduce a flux correcting factor f:

$$f(u = \cos[90 - \theta_{\rm apex}]; a, b) \quad = \quad \begin{cases} u^a & -1 \leq u < 0; \\ u^b & 0 \leq u \leq 1. \end{cases}, \qquad (2)$$

where $\theta_{\rm apex}$ and $\lambda_{\rm apex}$ are the polar and azimutal angle of the incoming direction with respect to the apex (direction of motion of the Earth). $a \approx 1$ and $b \approx 0.5$ are constants that we fit using the frequency as a function of apex angle of bolides in the NASA fireball database [1].

The number density of NEOs around a point $\vec{x} \equiv (q, e, i, \Omega, \omega)$ in configuration space is estimated with:

$$R(\vec{x}) \quad = \quad \sum_k W(||\vec{x} - \vec{x}_k||, h), \qquad (3)$$

where $||\vec{x} - \vec{x}_k||$ is a generalized "distance" and h a scale parameter. $W(||\vec{x} - \vec{x}_k||, h)$ is called the *smoothing kernel*, and it is intended to soft the transition from a discrete to a continuous regime (see Eq. 7 in ZS2018).

Distances in configuration space $||\vec{x} - \vec{x}_k||$ are computed using the Zappala et al. (1990) metric with the parametrization introduced by Rożek et al. (2011):

$$\begin{aligned} (D_Z/n_m a_m)^2 \quad = \quad & \tfrac{5}{4}(a - a_m)^2/a_m^2 + 2(e - e_k)^2 + \\ & + 2(\sin i - \sin i_k)^2 + \\ & + 10^{-4}(\Omega - \Omega_k)^2 + 10^{-4}(\varpi - \varpi_k)^2 \end{aligned} \qquad (4)$$

with $a_m = (a + a_k)/2$ the average semi-major axis between, n_m the corresponding orbital mean motion and $\varpi = \Omega + \omega$ the longitude of the perihelion.

4.1 Marginal Probabilities

In ZS2018, we sum-up the ray probabilities at a given geographical location, to compute the (relative) probability that an object impact that location instead of another one. This allows us to create maps of impact risk.

But ray probabilities can be used in different ways. Thus,

[1] https://cneos.jpl.nasa.gov/fireballs/

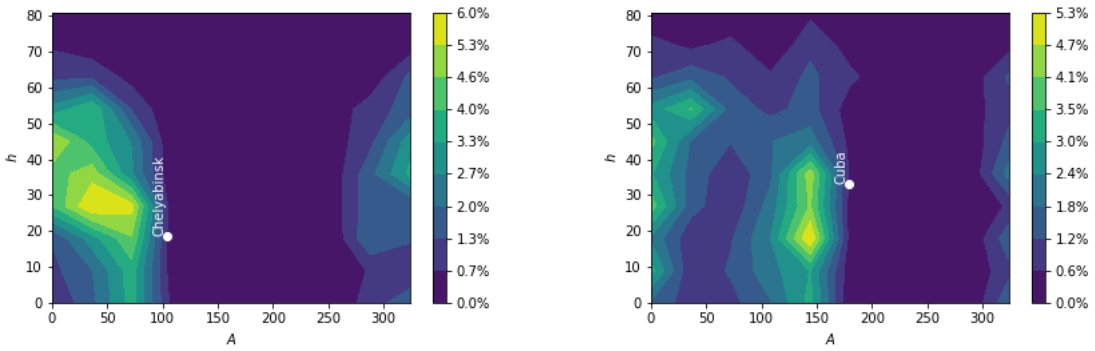

Figure 2. The estimated radiant for the Chelyabinsk (left panel) and Cuba meteor events (right panel), and the most prone meteoroid radiants in colourmaps according to the GRT technique.

for instance, we can estimate the probability distribution of impact speed, ie. $p(v_{\rm imp})\Delta v_{\rm imp}$, if we sum-up the ray probabilities having impact speeds in the interval $v_{\rm imp}, v_{\rm imp}+dv_{\rm imp}$:

$$p(v_{\rm imp})dv_{\rm imp} \propto \sum_{v_{\rm imp,i}\in[v_{\rm imp},v_{\rm imp}+dv_{\rm imp}]} P(A_i, h_i, v_{\rm imp,i}; t),$$

we call this the *marginal probability distribution* of $v_{\rm imp}$. The same rationale can be applied for computing the marginal probability distribution of any impact condition (radiant elevation, radiant azimuth, asymptotic orbit semi-major axis, etc.).

In Figure 1 we show the marginal probability distributions for several quantities of interest, as computed GRT at the location and time of the Chelyabinsk and Cuba event.

A similar approach can be generalized to compute two-dimensional marginal probability distributions. Thus, for instance, the probability that the radiant elevation and Azimuth be in the rectange $\mathcal{R}$: $[h_{\rm rad}, h_{\rm rad} + dh_{\rm rad}], [A_{\rm rad}, A_{\rm rad} + dA_{\rm rad}]$ will given by:

$$p(A_{\rm rad}, h_{\rm rad})dA_{\rm rad}dh_{\rm rad} \propto \sum_{h_{\rm rad,i}, A_{\rm rad,i}\in\mathcal{R}} P(A_i, h_i, v_{\rm imp,i}; t),$$

5 RESULTS

As we can notice in Figure 1, the observed impact conditions (speed and incoming directions), for both the Chelyabinsk and Cuba events, are within the statistical errors of the theoretical expectations obtained with GRT.

The case of the predicted azimuth is especially interesting. Although the observed value of this quantity in both events, have low marginal probability, GRT predicts the general direction in the sky from which the impactors arrived.

In the case of Chelyabinks, the GRT predicts a north-east radiant. In the real world, the object appeared coming from the east.

More interesting is the case of the Cuban meteoroid. The early records of the American Meteor Society, AMS[2] suggested a southbound incoming direction. The same direction was also suggested by one of the only videos of the event taken from a beach in Florida (see Supplementary Material). This direction, however, contradicted the GRT expectations of a northbound meteor (lower row in Figure 1) has a larger probability. This confuse our initial attempts to estimate the trajectory from the available footage. In the days after the event, new footage and satellite data, confirmed the fact that the meteor actually arrived from the south, as the GRT predicted.

To better understand the level of agreement between the GRT predictions and the observed impact conditions of these events, we plot in Figure 2 the joint marginal probability distribution of azimuth and elevation.

The color maps reveal details that are missing in the independent marginal probability distributions of azimuth and elevation. At the date, time and location of the Chelyabinsk event a spot around $A \sim 50°$ and $h \sim 25°$ has the largest probability. The actual meteor arrived not too far from there. In the Cuban case, two spots at an azimuth $A \sim 150°$, concentrate most of the expected incoming directions: one at a large elevation $h \sim 30°$ and a second one (and more probable) at low elevation $h \sim 20°$. The actual event happened close to the first spot.

The elements of the heliocentric orbit of the impactor, shows also interesting coincidences with those predicted by GRT. In Figure 3 we show joint marginal probability distribution for pairs of classical elements. For both events, the orbital elements of the impactor can be well-constrained by the theoretical preditions of GRT.

Especially noticeable are the case of inclination. For Chelyabinsk, GRT predicts a low inclination impactor with a moderate $e \sim 0.4-0.6$ eccentricity. The actual impactor has a $i \approx 5°, e \approx 0.6$ orbit. For Cuba, GRT anticipated relatively eccentric impactor $e \sim 0.6$ coming from a more inclined orbit $i \sim 8°$. The actual body had $i \approx 11°, e \approx 0.4$.

The longitude of the ascending node Ω seems to be easy to predict. It will mostly depend on the ecliptic longitude of the Earth at the time of impact. However the argument of the perihelion ω, namely the orientation of the axes of the ellipse in the orbital plane, is not as trivial to predict. Still, GRT anticipates reasonably well the value of ω for both events.

Interestingly, the orbit of the Chelyabinsk and Cuba im-

[2] https://fireball.amsmeteors.org/members/imo_view/event/2019/513

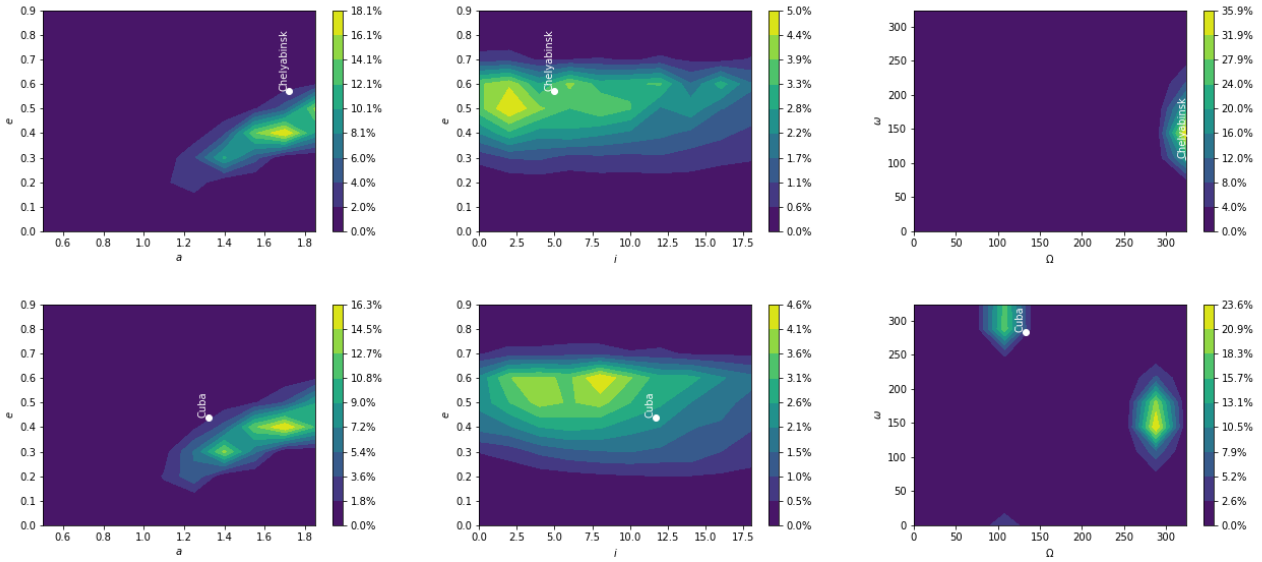

Figure 3. Colourmaps show the regions in the configuration (a, e, i, ω, Ω) space more prone to impact the Earth at the time and place of Chelyabinsk (uppermost panels) and Cuban meteors (lowermost panels).

pactors are similar. They have comparable eccentricities and inclinations. This may be explained by the fact that both impact happened in the same month and hence at a similar orbital position with respect to the NEOs distribution.

6 DISCUSSION

We started this letter by formulating a strong question: *Can we predict the impact conditions of meter-sized meteoroids??*. After examining the evidence presented here we propose a bold answer: *yes, we can predict them.*

But this answer should not surprise us. As the GRT method intrinsically assumes, the NEOs population acts like a gravitational "source of light" that instead of photons sends particles towards the Earth. Predicting the incoming impact direction is a simple consequence of knowing the properties of such body source.

Is GRT perfect and their predictions entirely reliable?. Probably not in its present version. As the differences between the predicted impact conditions and the observed ones seems to reveal, the method can be still improved. We should recall that this and the results in Zuluaga et al. (2019), are the first attempts to apply the method besides the test bench described in ZS2018. Better results could be obtained once we have a better knowledge of the NEOs distribution when new and more powerful surveys see their first light (Marshall et al. 2017). The method should also be improved from a theoretical point of view, but it is hard for a single group of authors to achieve it.

Being able to constraint impact conditions will not solve all the risks imposed by small undetectable objects. Still, it can help us to be prepared for future events, especially over populated areas. With this work, we also want to call the attention of governmental and no governmental institutions about the interest that theoretical research on impact risk assessment may have, and the potential that novel methods like GRT have at finding answer to what were considered unsolvable questions. We should implement real time programs for real time impact probability calculations, at least on the most populated cities on the world,

Our results here relied in our estimations of the Cuba meteor conditions. Although probably better values of those conditions, obtained after combining all the available information about the event, will be published in the near future, we are confident that the conclusions of this letter will not be substantially modified.

ACKNOWLEDGEMENTS

We have used NASA's ADS Bibliographic Services. Most of the computations that made possible this work were performed with NASA NAIF SPICE Software (Acton Jr 1996 and Jon D. Giorgini), `Python 2.7` and their related tools and libraries, `iPython` (Pérez & Granger 2007), `Matplotlib` (Hunter et al. 2007), `scipy` and `numpy` (Van Der Walt et al. 2011). We thank all the people in Cube who shared their videos and footage on the internet, for allowing us to reconstruct the Cuba meteor impact conditions. We are especially grateful to Rachel Cook who share its incredible video of the meteor from the Havana Harbor which was instrumental for the successful reconstruction of the trajectory. Karls Peña and Rafael Colon of the Dominican Astronomical Society Astrodom (the Dominican Republic) help us with the non-trivial task of finding information in Cuba about the meteor and the observation places, thanks to them for their effort.

REFERENCES

Acton Jr C. H., 1996, Planetary and Space Science, 44, 65
Borovička J., Spurnỳ P., Brown P., Wiegert P., Kalenda P., Clark D., Shrbenỳ L., 2013, Nature, 503, 235

Boslough M., Brown P., Harris A., 2015, in Aerospace Conference, 2015 IEEE. pp 1–12
Brown P., Spalding R. E., ReVelle D. O., Tagliaferri E., Worden S. P., 2002, Nature, 420, 294
Brown P., et al., 2013, Nature, 503, 238
Chapman C. R., 2004, Earth and Planetary Science Letters, 222, 1
Chapman C. R., Morrison D., 1994, Nature, 367, 33
Chesley S. R., 2005, Proceedings of the International Astronomical Union, 1, 215
Collins G. S., Melosh H. J., Marcus R. A., 2005, Meteoritics and Planetary Science, 40, 817
Comninos P., 2010, Mathematical and computer programming techniques for computer graphics. Springer Science & Business Media
Hills J. G., Goda M. P., 1998, Planetary and space science, 46, 219
Hunter J. D., et al., 2007, Computing in science and engineering, 9, 90
Marshall P., et al., 2017, arXiv preprint arXiv:1708.04058
Pérez F., Granger B. E., 2007, Computing in Science & Engineering, 9, 21
Popova O. P., et al., 2013, Science, 342, 1069
Rożek A., Breiter S., Jopek T., 2011, Monthly Notices of the Royal Astronomical Society, 412, 987
Rumpf C., Lewis H. G., Atkinson P. M., 2015, Conference Series
Silber E. A., Le Pichon A., Brown P. G., 2011, Geophysical Research Letters, 38
Svetsov V. V., Nemtchinov I. V., Teterev A. V., 1995, Icarus, 116, 131
Van Der Walt S., Colbert S. C., Varoquaux G., 2011, Computing in Science & Engineering, 13, 22
Zappala V., Cellino A., Farinella P., Knezevic Z., 1990, The Astronomical Journal, 100, 2030
Zuluaga J. I., Sucerquia M., 2017, in Revista Mexicana de Astronomia y Astrofisica Conference Series. pp 79–79
Zuluaga J. I., Sucerquia M., 2018, MNRAS, 477, 1970
Zuluaga J. I., Ferrin I., Geens S., 2013, arXiv preprint arXiv:1303.1796
Zuluaga J. I., Cuartas-Restrepo P. A., Ospina J., Pichardo F., Lopez S. A., Pena K., Gaviria-Posada J. M., 2019, arXiv e-prints, p. arXiv:1901.09573

Can we predict the impact conditions of meter-sized meteoroids?

Jorge I. Zuluaga, Pablo A. Cuartas-Restrepo, Jhonatan Ospina and Mario Sucerquia

APPENDIX A: SUPPLEMENTARY MATERIAL

A1 The 2019 Cuba meteor

The Cuba meteor happened in February 1, 2019 around 18:17 UTC. It was witnessed by thousands in the island and several casual observers in south Florida (USA). The meteor left a smoke trail and produced a sonic boom that recalled that of Chelyabinsk in 2013. According to the NASA fireball database [3] the meteor detonation released an estimated energy of 1.4 kt of TNT.

Here, we reconstruct the trajectory of the meteor in the atmosphere above Cuba and its orbit before the impact, using for that purpose different footage originally discovered and obtained from `YouTube`, `Instagram` and `Twitter`. In particular we analyzed three videos taken at different *vantage points*, both in Cuba and USA. Vantage points are separated by between 100 and 400 km ensuring a proper baseline for the reconstruction of the trajectory.

In Table A1 we present the position of the vantage points and links to the corresponding footage we use in our reconstruction.

A1.1 Havana observations

Havana observations are based in a Time lapse, recorded on board of a cruiser in the Havana Harbor. This video is the most complete and precise piece of footage publicly available about the event.

The video was taken using a `GoPro Hero 5` using the default Time Lapse mode (0.5 seconds between frames). We achieved to recover 11 frames spanning a total of 5 seconds, where the meteor is clearly visible.

Azimuth and elevation of the meteor were estimated by first identifying several reference buildings on the horizon (see upper panel in Figure A1).

A1.2 Florida observations

The second footage we use for our reconstruction is a video recorded by a camera of the `Earth Cam` network[4] in the top of the *Gull Wing Beach Resort* at Ft. Myers Beach, Florida (USA). A single frame of the video is shown in Figure A1.

Although the quality of the video is poor (as compared with that of the Havana) and the weather near to the Horizons was partially cloudy, we get enough information from the video to estimate the (relative) azimuth and elevation of the meteor.

To obtain the angular scale of the picture, we use as a reference object a truck (or container) apparently used for a jet ski station. The physical dimensions of the truck or container was obtained from a 3D model of the "truck" available in `Google Earth`. Combining the estimated distance between

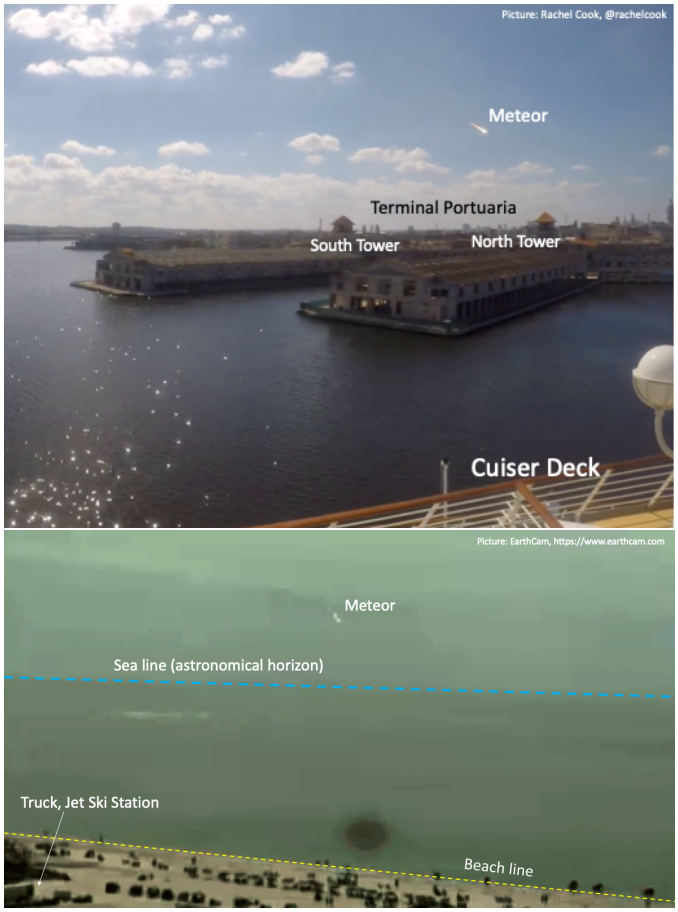

Figure A1. Upper panel: a single frame of the video taken in the Havana Harbor showing the reference buildings used in this work to estimate azimuth and elevation of the meteor. Lowe panel: frame of a video taken in the Gull Wing Beach Resort (Floria, USA).

the camera (which is located at the roof of the Resort) and the truck, we calculate the field of view of each pixel in the image. From that, we estimate the elevation of the meteor in each video frame.

Getting the azimuth of the meteor for this particular image was challenging. No fixed reference object could be identified along the beach. Therefore, our azimuth measurements were only relative to an arbitrary direction on the horizon. As we will see below, the precise azimuth of this reference direction was estimated a posteriori using the trajectory fitting procedure (Section A2.

A1.3 Pinar del Rio observations

The last footage we used for our reconstruction, was a street video showing the smoke trail left by the meteor. The video, recorded by a casual observer in the city of Pinar del Rio, 173 km to the west of Havana, was particularly well-suited for our purposes, in contrast with most videos recorded in the island, since it was plenty of reference objects able to provide us azimuths and the angular scale of the image. The video was apparently recorded a few minutes after the meteor. The site of the video was plenty identified in `Google Earth`.

We stitch together several of the frames in the video,

[3] https://cneos.jpl.nasa.gov/fireballs/
[4] https://www.earthcam.com/

Location	long. (deg)	lat. (deg)	alt. (m)	Public	Alternative
Havana Harbor, Cuba	-82.344343	23.13799	0	http://bit.ly/2GwIQqB	http://bit.ly/2UJ18c2
Gull Wing Beach Resrot, FL USA	-81.903714	26.419163	0	http://bit.ly/2tgUU7q	http://bit.ly/2TGGp8A
Alameda Pinar del Rio, Cuba	-83.692091	22.414536	48	-	http://bit.ly/2thGkMZ

Table A1. Location of the vantages points where the footage used in this work were taken. Public links are the original social network material. Alternative are permanent link to the footage.

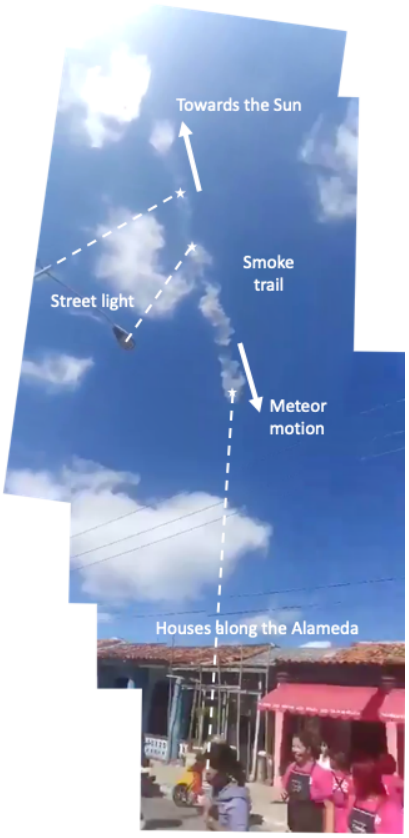

Figure A2. A single frame of the video taken from Pinar del Rio (Cuba), showing the hallmarks used in this work to estimate azimuth and elevation of the meteor.

showing the meteor trail and some reference objects, and the result is presented in Figure A2.

In order to get the elevation and azimuth of several points of the smoke trail, we first need to obtain the angular scale of the picture. For this purpose we use a lighting street pole located in the opposite side of the street. According to a source in the island, the height of the lighting street poles in Cuba is Standard. We use this height and the distance of the observer to the pole to gauge the angular scale of the pictures.

The scarce information available in the pictures about the meteor, only allows us to estimate the position of just three points in the smoke trail:

- the closest point to the top of a close lighting street pole (see Figure A2). The azimuth of this point was assumed the same as that of the pole (measured using `Google Earth`).
- The point in the smoke trail closer to the lamp in the street pole. The elevation of this point was obtained after estimating the position of the zenith using the first measurement. A line drawn from the zenith to the lamp allows us to estimate the distance and hence the angle between the lamp and the smoke trail point. The azimuth of this line is the same as the azimuth of the vertical to the lamp as seen from the location of the observer. The elevation of the lamp was estimated from the distance between the lamp and the observer.
- The lowest point of the trail. The azimuth of this point was estimated using as references the roof of houses below the trail. `Google Earth`provided us the azimuth of those houses. The elevation was estimated using the angular distance between the trail and the ground.

The previous procedure has large uncertainties (several degrees in most of the cases) and it relies mostly on unknown properties (the height of the light pole, the azimuth of the houses, etc.) Moreover, this procedure give us the observed coordinates of the smoke trail and not of the meteor itself. Still, in the absence of other more reliable visual recording inside the island, the information provided by this images are priceless.

In Table A2 we summarize the observed coordinates (azimuth and elevation) of the meteor as estimated with the aforementioned procedures for the three vantage points.

A2 Trajectory fitting

One of the main limitations of working with public or amateur footage is the lack of a proper synchronization among videos. In only two of them (the Havana and Florida videos) we have information about the time of each frame relative to the beginning of the video (last column in Table A2). No absolute timing was available.

For solving this inconvenience we developed in Zuluaga et al. (2013) a numerical procedure intended to fit a meteor trajectory, starting only with the measurements of elevations and azimuths. We call it the "Altazimuth-footprint method".

In contrast with the original version of the method, the improved version we use here, involved both, errors in elevation and azimuth to compute the altazimuth-footprint statistics:

$$\mathcal{A} = \sqrt{\sum_{j=1}^{n_v}\sum_{i=1}^{n_j}\left[\frac{(A_{ji}-A_{tji})^2}{\Delta A_{ji}^2}+\frac{(h_{ji}-h_{tji})^2}{\Delta h_{ji}^2}\right]} \tag{A1}$$

Here, n_v is the number of vantage points, n_j is the number of observations in the jth vantage point, (A_{ji}, h_{ji}) are the horizontal coordinates of the ith point in the jth vantage point, and (A_{tji}, h_{tji}) are the azimuth and elevation of the closest point in the theoretical trajectory respectively.

Point	Az. (deg)	h (deg)	t (s)
Havana harbor			
1	223.97 ± 0.02	19.3 ± 0.08	0.00
2	225.42 ± 0.02	18.5 ± 0.08	0.50
3	226.94 ± 0.02	17.7 ± 0.08	1.00
4	228.67 ± 0.02	16.7 ± 0.08	1.50
5	230.26 ± 0.02	15.6 ± 0.08	2.00
6	232.12 ± 0.02	14.7 ± 0.08	2.50
7	233.98 ± 0.02	13.6 ± 0.08	3.00
8	235.91 ± 0.02	12.3 ± 0.5	3.50
9	237.99 ± 0.02	11.0 ± 0.5	4.00
10	240.09 ± 0.02	9.6 ± 0.5	4.50
11	242.04 ± 0.02	8.3 ± 0.5	5.00
GullWing Beach Resort (Florida)			
1	$A_{\rm ref}$+10.1 ± 0.1	2.5 ± 0.3	0.44
2	$A_{\rm ref}$+10.2 ± 0.1	2.3 ± 0.3	0.50
3	$A_{\rm ref}$+10.5 ± 0.1	2.0 ± 0.3	0.81
4	$A_{\rm ref}$+10.8 ± 0.1	1.6 ± 0.3	0.94
5	$A_{\rm ref}$+11.2 ± 0.1	1.1 ± 0.3	1.94
6	$A_{\rm ref}$+11.5 ± 0.1	0.8 ± 0.3	2.31
Pinar del Rio (Cuba)			
1	287.61 ± 0.1	76.9 ± 5	-
2	308.32 ± 5	68.2 ± 5	-
3	318.07 ± 5	57.8 ± 5	-

*$A_{\rm ref}$ is obtained in the fitting procedure.

Table A2. Observed trajectory of the meteor in the sky as estimated in this work for three different vantage points.

The theoretical trajectory depends on four quantities: the projected impact site location ($\rm lon_{imp}$,$\rm lat_{imp}$) ($\rm alt_{imp}$=0), the radiant azimuth $A_{\rm rad}$ and the radiant elevation $h_{\rm rad}$ as seen from the projected impact site.

In order to find the best-fit value of those parameters we minimize the statistics $\mathcal{A}$. Due to the particularities of the Florida footage, we add a fifth parameter to the minimization procedure, namely the reference Azimuth $A_{\rm ref}$ at the Gull Wing Beach vantage point (see Table A2).

The result of the fitting procedure is presented in Table A3. Using the best-fit trajectory, we also compute the heliocentric orbit of the meteoroid 1 year before the impact. The resulting classical elements are also shown in this Table.

A plot with a comparison between the observed meteor trajectory and the best-fit Altazimuthal footprint, is presented in Figure A3.

We found that in order to explain our three visual observations, the object should come almost exactly from the south, traveling in an inclined $h_{\rm rad}$ = 33° trajectory towards the north coast of Cuba. According to the observations in the Havana Harbor the contact point of the object with the atmosphere happened at 76 km above the ocean to the south of San Felipe Cays. The brightest point in the video corresponds to a point in the trajectory 27 km obove the surface.

On the other hand, according to our estimations, the smoke trail seen in the Pinar del Rio video, corresponds to a short segment of the trajectory between 26 km and 22.5 km. The latter point, apparently correspond to the end of the airburst.

Using our fitted trajectory and the very precise footage taken at the Havana harbor, we can estimate the distance traveled by the meteoroid in the atmosphere as a function of time. A linear regression of the resulting distances, provide us the average speed of the meteoroid during the airburst.

We see that the speed of the meteoroid was almost constant between 76 km and 26 km height, and started to decrease just after that moment.

Parameter	Best fit value
Atmospheric trajectory	
Lon. impact (deg)	-83.78217648 ± 0.05
Lat. impact (deg)	22.80238773 ± 0.05
$A_{\rm rad}$ (deg)	$179\ ^{+1}_{-4}$
$h_{\rm rad}$ (deg)	$33\ ^{+0.5}_{-1.5}$
$A_{\rm ref}$ (deg)	192.5 ± 0.5
$\langle v_{\rm imp} \rangle$ (km/s)	$18.0\ ^{+0.3}_{-1.2}$
Orbit	
a (AU)	$1.32^{+0.06}_{-0.06}$
q (AU)	$0.75^{+0.02}_{-0.02}$
e (AU)	$0.44^{+0.02}_{-0.02}$
i (AU)	$11.68^{+0.4}_{-0.4}$
Ω (AU)	$132.54^{+0.004}_{-0.003}$
ω (AU)	283.77^{+3}_{-5}
P (yr)	$1.52^{+0.1}_{-0.1}$
T_p (adim.)	$2.78^{+0.02}_{-0.02}$

Table A3. Best-fit values of the atmospheric trajectory and the asymptotic orbit of the meteoroid for the Cuba impact as estimated in this work.

A3 Discussion

The estimated impact conditions, presented here, depends on several assumptions and on the validity of the geometrical procedures used to measure azimuths and elevations over the pictures.

The most uncertain measurements are those taken at Pinar del Rio. Since the footage there does not include the visible meteor but the smoke trail, it could happen that the cloud be displaced from the actual meteor trajectory by several degrees. In particular the meteor could happen to the west of the cloud observed position. In this case the trajectory will be farther away from the Havana Harbor and hence the estimation of the distance traveled by the meteoroid, and hence the impact speed, will also be affected.

We have played around with the observed coordinates of the Pinar del Rio observations, modifying elevations and azimuths to simulate the effect of the wind. The errors reported in Table A3 reflect those uncertainties.

In order to estimate the errors in the orbital elements, we create 1000 test particles having random impact conditions within the intervals defined by the errors in the atmospheric trajectory section of Table A3. The errors reported in the orbital elements are the result of this simulations. We noticed that even if, for instance the impact speed is as low as 16.8 km/s (the lowest velocity allowed by our footage), the orbital elements are not significantly modified.

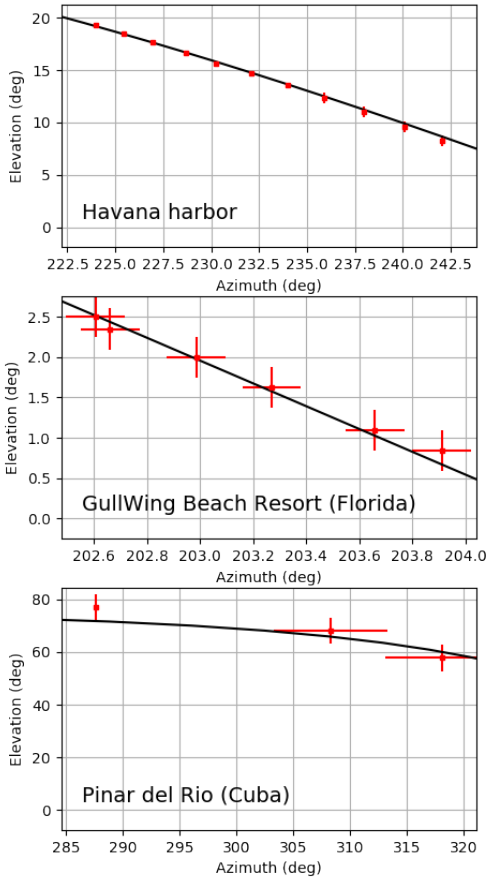

Figure A3. Expected azimuth and elevation of the theoretical trajectory (continuous line) as observed from the vantage points, and the actual measurements estimated in this work. In the three cases the horizontal and vertical ranges have been adjusted to the ranges of the available data.

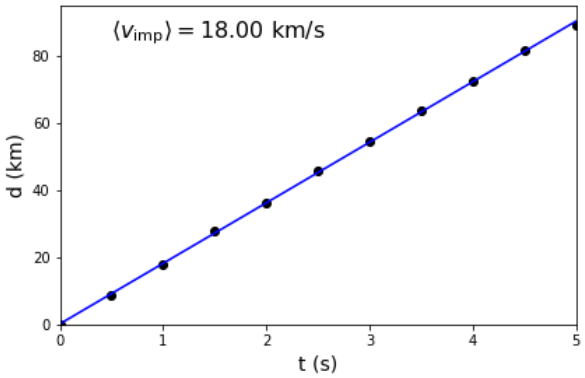

Figure A4. Distance travelled by the meteor using the best-fit trajectory and the Havana Harbor observations (black dots). The blue line corresponds to the linear regression. The average impact speed $\langle v_{\rm imp} \rangle$ corresponds to slope of the blue continuous line.

A4 Reproducibility

In order to make all our results reproducible, we provide all the input data, simulation results, spreadsheets and crude videos and images, in a public `GitHub` repository: `http://github.com/seap-udea/MeteorTrajectories.git`. The GRT method was implemented in a `C++/python` package also publicly available in the `GitHub` repository `http://github.com/seap-udea/GravRay.git` (branch `MoonImpact`).

Any suggestion, observations or corrections will be greatly appreciated.

This paper has been typeset from a TEX/LATEX file prepared by the author.